



Dual-energy computed tomography-based volumetric thyroid iodine quantification: correlation with thyroid hormonal status, pathologic diagnosis, and phantom validation

Younghen Lee

Korea University College of Medicine, Ansan Hospital,
Department of Radiology, Ansan, South Korea

PURPOSE

To investigate the relationship between intrathyroidal iodine concentration (IC) (mg I/mL) and thyroid hormonal status or pathologic diagnosis with the use of dual-energy computed tomography (DECT).

METHODS

We retrospectively included patients who underwent neck CT examination between September 2016 and August 2021 using a dual-layer DECT scanner (120 kilovolt peak) for preoperative thyroid imaging. We performed volumetric IC measurements at the thyroid parenchyma on the additional iodine map generated from non-contrast images. We then compared the mean IC of thyroid parenchyma based on thyroid hormonal status (hypothyroid, euthyroid, and hyperthyroid) and diffuse thyroid disease (DTD). Additionally, we determined the accuracy of iodine quantification with our site-specific DECT acquisition protocol using a Gammex™ phantom containing seven iodine inserts with different ICs ranging from 2 to 20 mgI/mL.

RESULTS

Among the 578 patients (M:F: 87:491, age: 48.6 ± 11.7 years) who were finally selected, the mean thyroid parenchymal ICs was the lowest in the hyperthyroid group, followed by the hypothyroid group, and then the euthyroid group (0.68 ± 0.37 , $n = 44$ vs. 1.13 ± 0.42 , $n = 61$ vs. 1.32 ± 0.43 , $n = 473$, $P < 0.01$, respectively). In the patients with euthyroidism, the mean parenchymal IC was already lower in the patients with pathologically proven DTD than in those without DTD (1.22 ± 0.44 mgI/mL vs. 1.45 ± 0.37 mgI/mL, $P < 0.01$). Based on the phantom study, the median percentage deviations from the expected values were 5.1% for ICs of 2–20 mgI/mL.

CONCLUSION

DECT-based IC quantification could be a potentially useful method for identifying patients with thyroid hormone dysfunction or DTD without the use of contrast media.

CLINICAL SIGNIFICANCE

Without the need for intravenous administration, DECT-based intrathyroidal IC quantification provides potentially valuable information from the non-contrast CT image of the thyroid parenchyma

KEYWORDS

Thyroid gland, dual-energy computed tomography, iodine concentration, hyperthyroidism, hypothyroidism, hormone

Corresponding author: Younghen Lee

E-mail: younghen@korea.ac.kr

Received 21 November 2024; revision requested 16 January 2025; accepted 04 February 2025.



Epub: 18.03.2025

DOI: 10.4274/dir.2025.243132

In non-contrast computed tomography (CT) imaging, the normal thyroid gland, which harbors approximately 70%–80% of the body's iodine in a healthy adult,¹ exhibits a distinctive increase in CT attenuation in comparison with other anatomical structures. In contrast, patients presenting with thyroid hormone dysfunction or underlying thyroiditis exhibit a pronounced reduction in CT attenuation, suggestive of inflammatory cell infiltration within the thyroid gland.^{2–6} It is crucial to acknowledge that CT attenuation is not a fixed measurement; rather, it is susceptible to fluctuations influenced by technical parameters, including the type

of scanner employed, tube potential [kilovolt peak (kVp)], and patient positioning.^{7,8} These factors can markedly amplify the observed changes in the thyroid gland, which is particularly rich in iodine. Moreover, X-ray fluorescence spectrometry has emerged as a novel technique for evaluating the intrathyroidal iodine pool.^{9,10} However, it is limited to the analysis of formalin-fixed samples and, as a result, is not applicable for individual patient assessments.

Previous research utilizing dual-energy CT (DECT) has shown the ability to directly measure iodine concentration (IC) from individual voxels. This advancement has enhanced diagnostic performance in oncological imaging by facilitating the prediction of pathological subtypes, assessing post-treatment responses, and determining prognosis.¹¹⁻¹³ Recent studies have suggested that measuring IC obtained through DECT could be advantageous in the treatment of patients with thyroid hormone disorders.¹⁴⁻¹⁶ However, these studies did not sufficiently consider the impact of thyroid hormone status or the technical parameters associated with DECT. Consequently, the present study investigates the feasibility of quantifying iodine from non-contrast thyroid CT images of patients with established thyroid hormone status and/or histopathological diagnoses, in addition to using a CT phantom containing iodine inserts, through the application of recently developed dual-layer detector DECT technology.

Methods

This study was approved by the Korea University Ansan Hospital Institutional Review Board and the requirement of informed consent was waived due to its retrospective chart review and image analysis (approval no: AS20180180, date: September 2023).

Patient population

To evaluate the parenchymal IC of the entire thyroid gland using non-contrast CT images in relation to thyroid function and pathological findings, we conducted a retrospective analysis of the medical records of 1,365 patients who underwent neck CT examinations using a DECT scanner at our institution between September 2016 and August 2021. The criteria for inclusion in this study were as follows: (a) the entire thyroid gland was imaged without the use of contrast media during the neck CT examination; (b) thyroid hormone levels, including free thyroxine (fT4) (ng/dL), triiodothyronine (T3) (ng/dL), and thyroid-stimulating hormone (TSH) (uIU/mL), were measured within 1 month prior to the CT examination; (c) any thyroid nodule present had a diameter of ≤10 mm as determined by sonographic imaging or final surgical specimens, if surgery was performed; (d) patients had no prior history of medication that could potentially influence thyroid function test results, such as dopamine agonists, glucocorticoids, somatostatin analogues, metformin, salicylates, phenytoin, lithium, and tyrosine kinase inhibitors; and (e) the overall quality of the CT images was not significantly compromised by beam-hardening artifacts, primarily associated with adjacent bony structures.

Finally, a total of 578 patients (M:F: 87:491, mean age: 48.6 ± 11.7 years) were included for DECT-based IC quantification. Comprehensive patient characteristics are presented in Table 1 and Figure 1. The primary indication for neck CT in these patients was preoperative planning, particularly concerning neck lymph node metastasis.¹⁷ As such, non-contrast CT images were routinely acquired before contrast administration to identify calcifications or cystic change in neck lymph nodes, which are well-established CT indicators of metastatic thyroid carcinoma.¹⁷

According to the TSH results, 61, 473, and 44 patients were classified as hypothyroid, euthyroid, and hyperthyroid, respectively. The mean age and sex distribution did not differ across the three groups (all *P* > 0.05). The TSH levels were significantly different across the three groups (all *P* < 0.01), whereas a significant difference existed only between the hyperthyroid group and the other two groups for the fT4 and T3 levels (all *P* < 0.01). Among the 521 patients who underwent total thyroidectomy, subtotal thyroidectomy, or hemithyroidectomy for the removal of thyroid nodules with cytological diagnoses or to alleviate symptoms associated with hyperthyroidism, 318 patients were pathologically diagnosed with diffuse thyroid disease (DTD).

Data acquisition and iodine quantification

Non-contrast CT images utilized for the quantification were obtained using a single-source, dual-layer detector CT system (Philips Healthcare, IQon Spectral CT scanner, Cleveland, OH, USA). The imaging parameters employed included a tube voltage of 120 kVp, a mean tube current of 42 mAs (with a range of 30–150 mAs), a collimation thickness of 64*0.625 mm, a helical pitch of 0.609, a rotation time of 0.75 seconds per rotation, and a field of view measuring 350 mm. The scan encompassed a range from the skull base to the aortopulmonary window. An automatic tube current modulation system was engaged during the scanning process along both the X-Y and Z axes (DoseRight 3D-DOM; Philips Healthcare).

All acquired images were subsequently transferred to and analyzed using specialized DECT postprocessing software (Spectral Diagnostic Suite version 6.5, Philips Healthcare) to generate an iodine-specific density map through projection-based material

Main points

- Dual-energy computed tomography (CT) can quantify the inherent thyroid iodine status using the non-contrast CT images
- The intrathyroidal iodine concentration (IC) was observed to be significantly reduced in patients exhibiting hypo- or hyperthyroidism in comparison with those with euthyroidism, with a reference range determined to be 1.32 ± 0.43 mgI/mL.
- Significantly decreased intrathyroidal IC was observed in patients with pathologically confirmed diffuse thyroid disease, even in those who are euthyroid.

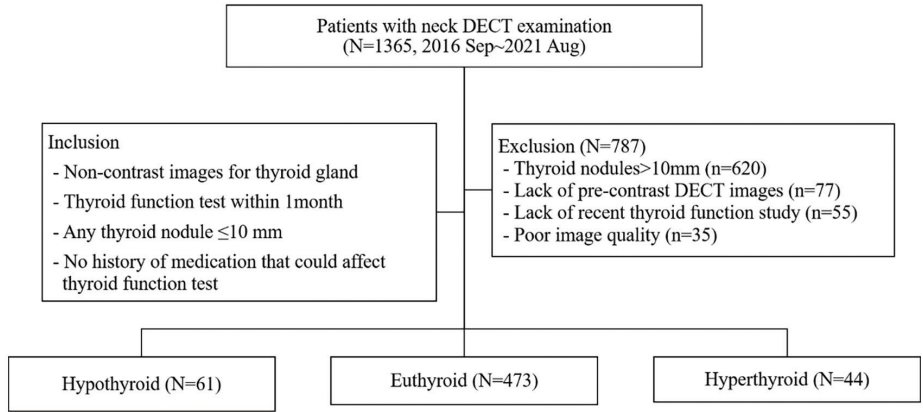


Figure 1. Flowchart of included patients with dual-energy computed tomography-based thyroid gland iodine quantification. DECT, dual-energy computed tomography.

Table 1. Clinical characteristics of the patients				
	Hypothyroid	Euthyroid	Hyperthyroid	P value
Numbers of patients (men: women)	61 (9:52)	473 (72:401)	44 (6:38)	>0.05*†
Age (years)	50.4 ± 10.3	48.3 ± 11.4	48.5 ± 15.8	>0.05*†
Thyroid-stimulating hormone (uIU/mL, normal range: 0.17–4.05)	5.94 ± 1.44	1.74 ± 0.83	0.04 ± 0.04	<0.01*†
Free thyroxine (ng/dL, normal range: 0.79–1.86)	1.21 ± 0.17	1.29 ± 0.15	1.56 ± 0.56	<0.01*†
Triiodothyronine (ng/dL, normal range: 78–182)	116.4 ± 33.6	115.8 ± 32.8	150.5 ± 56.6	<0.01*†
Numbers of pathologic diagnosis for thyroid parenchyma (no pathologic results: normal: diffuse thyroid disease)	6:14:41	36:189:248	15:0:29	

Data shown as mean ± standard deviation. The presented P values resulted from comparison between three groups with different thyroid hormonal status, using chi-squared tests for categorical variables and one-way analysis of variance tests for continuous variables. *, hypothyroid vs. euthyroid; †, hypothyroid vs. hyperthyroid; ‡, euthyroid vs. hyperthyroid.

decomposition.⁷ Conventional images were reconstructed employing a hybrid iterative reconstruction algorithm (iDose 4, level 3) alongside a soft tissue algorithm [window level set at 60 Hounsfield unit (HU); window width at 300 HU], with a slice thickness of 2 mm.

For the volumetric assessment of CT attenuation values and IC in the thyroid glands, a board-certified radiologist with 19 years of expertise in head and neck imaging utilized a semi-automated region-growing technique to encompass the entire thyroid gland on 40-kiloelectronvolt (keV) virtual monoenergetic images, as this kiloelectron volt level significantly enhances intrathyroidal iodine CT attenuation.^{7,8} Additional sets of iodine density maps and conventional images were

employed to derive IC and CT attenuation values (Figure 2). The total thyroid volume, inclusive of both lobes and the isthmus, was calculated. Measurements were conducted three times using the vendor's proprietary image viewer (IntelliSpace Portal v9; Philips Healthcare) and subsequently averaged.

Hormone status and pathologic analysis

The thyroid hormone status of patients was categorized into three distinct groups: hypothyroid, euthyroid, and hyperthyroid, based on recent serum levels of TSH and fT4. The reference ranges utilized by our institution were as follows: TSH levels between 0.17 and 4.05 uIU/mL and fT4 levels between 0.85 and 1.86 ng/dL. TSH is recognized as the most effective screening mark-

er for thyroid function due to its enhanced sensitivity and specificity relative to other hormonal assessments.¹⁸ Accordingly, in this study, patients were classified into the hypothyroid, euthyroid, and hyperthyroid groups based on their TSH levels being above the upper limit, within the reference range, or below the lower limit of the reference range, respectively. Additionally, for patients who underwent thyroid surgery at our institution, we documented the pathological subtypes of thyroid nodules and the presence of DTD, which encompasses a diverse array of autoimmune inflammatory or hyperplastic conditions, including Hashimoto's thyroiditis (HT) and nodular or diffuse hyperplasia.¹⁹

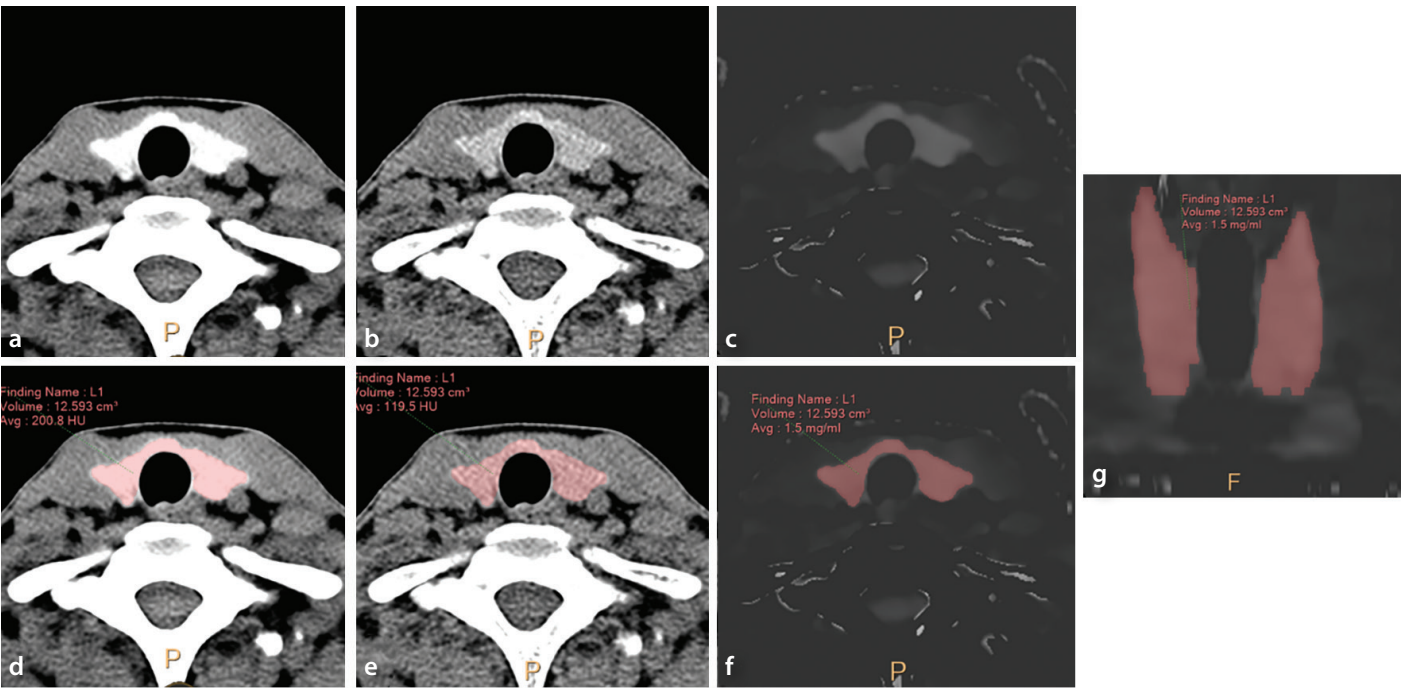


Figure 2. Example of thyroid parenchymal iodine concentration (IC) measurement. Initially, the volumetric region of interest encompassing the entire thyroid glands was drawn on the axial 40-keV virtual monoenergetic images (a, d) using the semi-automated region-growing method. Then, both mean CT attenuation value and IC were obtained from the corresponding iodine density map (c, f, g) and conventional CT images (b, e). Total thyroid volume was also recorded. keV, kiloelectronvolt; CT, computed tomography.

Statistical analysis

Categorical variables represented numerically were analyzed across the three groups (euthyroid, hypothyroid, and hyperthyroid) using the chi-squared test. Continuous variables were reported as mean ± standard deviation or median (interquartile range). To assess the differences in parenchymal CT attenuation, IC, and total thyroid volume among the three distinct thyroid hormone groups, one-way analysis of variance (ANOVA) was conducted following the verification of normal distribution through the Shapiro–Wilk test. The Bonferroni correction was applied to account for multiple comparisons. Additionally, a subgroup analysis was performed on the euthyroid group to evaluate the presence or absence of DTD in their surgical specimens. The relationship between continuous variables (IC, CT attenuation, age, fT4, and TSH) was examined using bivariate Pearson or Spearman correlation analysis. Data analysis was conducted using IBM SPSS Statistics 25.0 (Armonk, NY, USA), with a *P* value of <0.05 deemed indicative of a statistically significant difference.

Phantom study

To evaluate the quantitative accuracy of the DECT protocol for IC calculation, we employed an electron density phantom (Gammex™ 467, Gammex Inc., Middleton, WI, USA) that contained iodine-loaded inserts (2.8 cm in diameter and 7 cm in length) corresponding to seven different ICs (2.0, 2.5,

5.0, 7.5, 10.0, 15.0, and 20.0 mgI/mL), in addition to a solid water insert rod, positioned within the inner circle of the phantom, while the outer ring remained unfilled.^{11,12,20} During the scanning process, the phantom was axially aligned on the scanner table and centered within the gantry to facilitate axial scans of the insert-filled section of the phantom (Figure 3). The CT parameters selected were consistent with our standard protocol for adult neck scans, using a voltage of 120 kVp. Both conventional and spectral base images were generated for subsequent analysis, following the methodology previously described. Circular regions of interest (ROIs) measuring approximately 100 mm² were delineated at the center of each insert across 10 consecutive slices. Each scan was conducted three times, resulting in a total of 30 measurements for each rod. The analysis of measured versus expected values included the calculation of the absolute difference (measured–expected) and the percentage deviation, expressed as [100 × (measured– expected)/expected].

Results

Mean intrathyroidal iodine concentration values in the three different thyroid hormonal groups

The means of CT attenuation values, IC, total volume, and iodine content of the whole thyroid glands are summarized in Table 2. In the group of 473 patients with euthyroidism, the means of CT attenuation values, IC, and total volume of thyroid parenchyma were

103.2 ± 16.5 HU, 1.32 ± 0.43 mgI/mL, and 11.7 ± 11.9 mL, respectively. Based on ANOVA tests, mean intrathyroidal CT attenuation values and IC were significantly different among the three groups (all *P* < 0.01). Mean CT attenuation values and IC were the lowest in the hyperthyroid group, and lower in the hypothyroid group compared with the euthyroid group (0.68 ± 0.37 mgI/mL, 75.2 ± 19.3 HU vs. 1.13 ± 0.42 mgI/mL, 95.1 ± 18.2 HU, all *P* < 0.01) (Figure 4). Furthermore, the hyperthyroid group presented with a significantly larger thyroid volume compared with both the euthyroid group and the hypothyroid group (all *P* < 0.05); however, no statistically significant difference in volume was observed between the euthyroid and hypothyroid groups (*P* > 0.05).

Difference in intrathyroidal iodine concentration values based on pathologic diagnosis

In the group of 437 patients with euthyroidism who underwent thyroid surgery, the mean thyroid parenchymal IC was found to be significantly lower in those diagnosed with DTD in comparison to those without this diagnosis, as confirmed by pathological assessment (1.22 ± 0.44 mgI/mL vs. 1.45 ± 0.37 mgI/mL; *P* = 0.023, Figure 5).

Correlation between intrathyroidal iodine concentration values and other continuous variables

Using Pearson correlation analysis, thyroid parenchymal IC had a statistically sig-

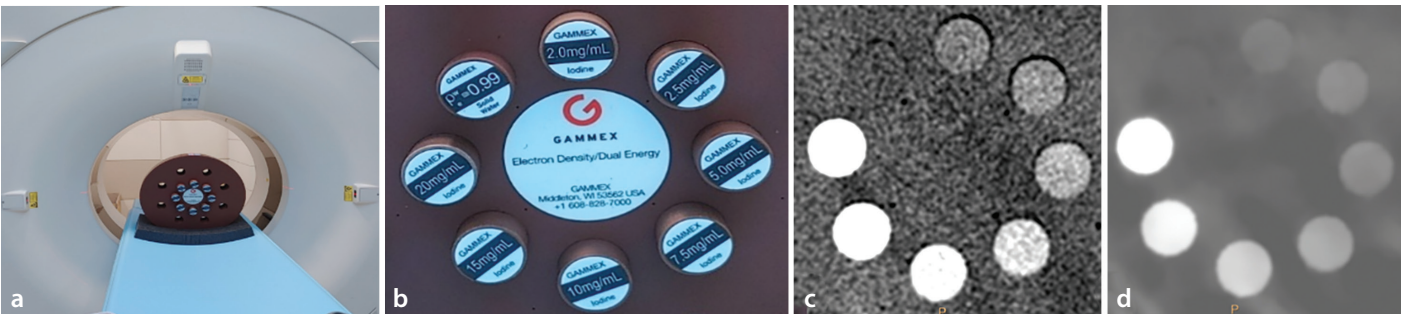


Figure 3. Gammex phantom with different iodine concentrations. To examine the accuracy of iodine quantification using dual-energy computed tomography (CT), iodine concentration increased clockwise from 12 o'clock position (a, b). The zoom-in conventional axial CT image [(c): window level/width 60/300 HU] and iodine density map [(d): window level/width 3/15 mgI/mL] acquired with 120 kVp show the increased signal. kVp, kilovolt peak; HU, Hounsfield unit.

Table 2. Volumetric quantification of entire thyroid glands with different thyroid hormonal status using dual-energy computed tomography datasets				
	Hypothyroid (n = 61)	Euthyroid (n = 473)	Hyperthyroid (n = 44)	<i>P</i> value
Computed tomography attenuation (HU)	95.1 ± 18.2	103.2 ± 16.5	75.2 ± 19.3	<0.01*†‡
Iodine concentration (mgI/mL)	1.13 ± 0.42	1.32 ± 0.43	0.68 ± 0.37	<0.01*†‡
Total volume of thyroid gland (mL)	11.2 ± 7.1	11.7 ± 11.9	46.3 ± 59.0	<0.05†‡

Data shown as mean ± standard deviation. *, hypothyroid vs. euthyroid; †, hypothyroid vs. hyperthyroid; ‡, euthyroid vs. hyperthyroid; HU, Hounsfield unit.

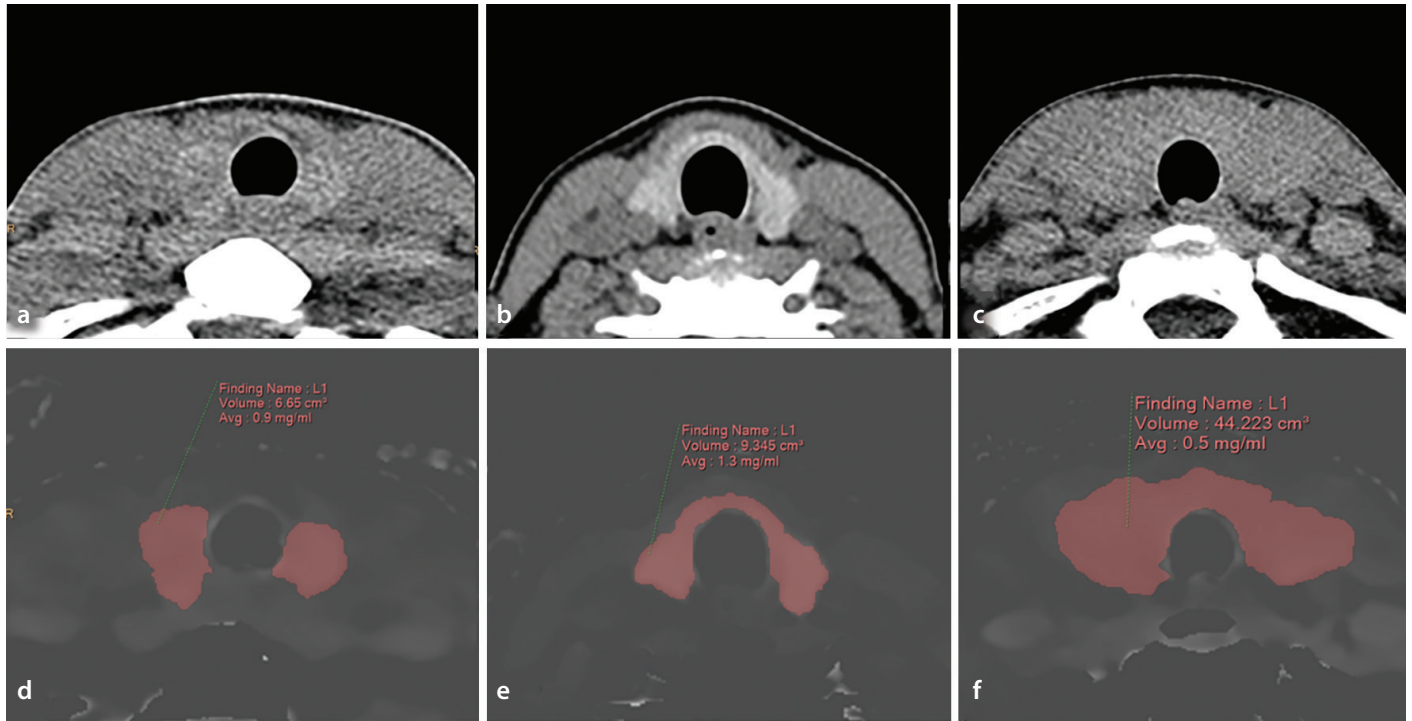


Figure 4. Representative non-contrast computed tomography (CT) images of thyroid gland in the patients with different thyroid hormonal status. The region of interest-indicated iodine density maps (d-f) switched from the upper conventional CT images [(a): hypothyroid, (b): euthyroid, (c): hyperthyroid] show the significantly decreased mean thyroid parenchymal iodine concentration in the patients with hypo-/hyperthyroidism than the euthyroid group (0.9, 0.5 mgI/mL vs. 1.3 mgI/mL).

nificant strong positive relationship with CT attenuation only ($r = 0.859$, $P < 0.01$), whereas other variables, including age, fT4, and TSH, had no relationship with thyroid parenchymal IC ($r = -0.033$, -0.069 , 0.054 , respectively, all $P > 0.05$).

Accuracy of iodine quantification using computed tomography phantom

Examples of conventional CT and IC images of iodine inserts using the same scanning protocol implemented at our institution for the acquisition of non-contrast DECT images are shown in Figure 6. The quantification results for the iodine inserts indicated good agreement between the individual measurement values and the reference values, yielding an overall median difference of 0.36 mgI/mL (range: 0.12–0.58 mgI/mL) and a mean percentage deviation of 5.1% (range: 2.2%–6.2%) for IC values between 2.0 and 20.0 mgI/mL.

Discussion

This study presents the first reference range of intrathyroidal IC of patients with euthyroidism from non-contrast thyroid CT images using DECT-based IC quantification. As anticipated, the mean intrathyroidal IC values were significantly lower in patients with hypo-/hyperthyroidism when compared

with those who were euthyroid. Furthermore, the observed decrease in IC associated with concurrent DTD occurred prior to the onset of thyroid hormonal dysfunction. Consequently, the reference range for intrathyroidal IC provided in this study will enhance the understanding of iodine metabolism in the context of thyroid hormone disorders.

Iodine is a crucial micronutrient required for the synthesis of thyroid hormones.²¹ In healthy adults, the sodium/iodine symporter facilitates the active transport of iodide into the thyroid follicles, operating across a concentration gradient that is 20–50 times greater than that found in plasma. Consequently, a substantial proportion of iodine, estimated at 70%–80% (equivalent to 15–20 mg), is sequestered in colloid pools.¹ These pools exert a predominant effect on the CT attenuation values of the thyroid gland. Previous experimental studies have demonstrated a direct relationship between CT attenuation and IC in solution, supporting the use of intrathyroidal CT attenuation as a functional indicator for the early detection and assessment of thyroid disease severity.^{3–6} However, iodine, an element with a high atomic number ($Z = 53$), exhibits variable CT attenuation depending on the photon energy level, especially just beyond its K-edge (33.2 keV).^{7,8} As a result, the manipulation of iodine CT attenuation can be achieved through adjustments

in kVp. Furthermore, neighboring osseous structures often result in significant beam hardening artefacts in the vicinity of the thyroid gland, impeding the precision of CT attenuation.

To overcome these problems in CT attenuation measurement, several researchers have advocated for DECT-based IC quantification as a more precise and dependable diagnostic approach for evaluating thyroid hormone levels.^{14–16} Binh et al.¹⁴ were the first to propose the use of intrathyroidal IC as a functional marker in patients with hyperthyroidism, demonstrating a significant negative correlation between iodine 123 uptake at 3 hours and intrathyroidal IC ($r = -0.680$, $P < 0.05$). However, no correlation was found between iodine 123 uptake and CT attenuation values ($P = 0.087$).¹⁴ In a study involving 226 patients with euthyroidism, it was observed that intrathyroidal IC was significantly lower in men compared with women and exhibited a gradual decline in patients over the age of 40.¹⁵ Another investigation involving patients with euthyroidism revealed that mean IC and total iodine content were positively correlated with fT3/total-T3 levels, but exhibited a negative correlation with TSH.¹⁶ However, prior studies measured intrathyroidal IC values at only two or three slices of each lobe, averaging the results without assessing the entire thyroid volume.^{14–16} Ad-

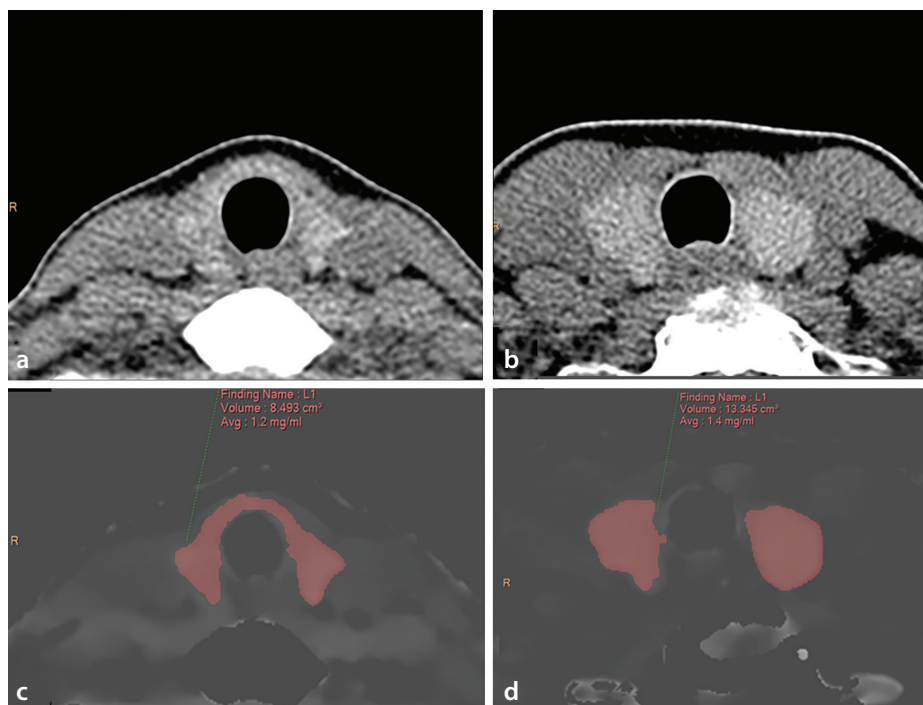


Figure 5. Non-contrast computed tomography (CT) image characteristics in the euthyroid group patients with and without diffuse thyroid disease (DTD). Compared with the conventional CT images of thyroid gland (a, b), the reduced intrathyroidal iodine concentration and total thyroid volume were confirmed in patients with DTD by iodine quantification [(c): 1.2 mgI/mL with 8.5 mL vs. (d): 1.4 mgI/mL with 13.3 mL].

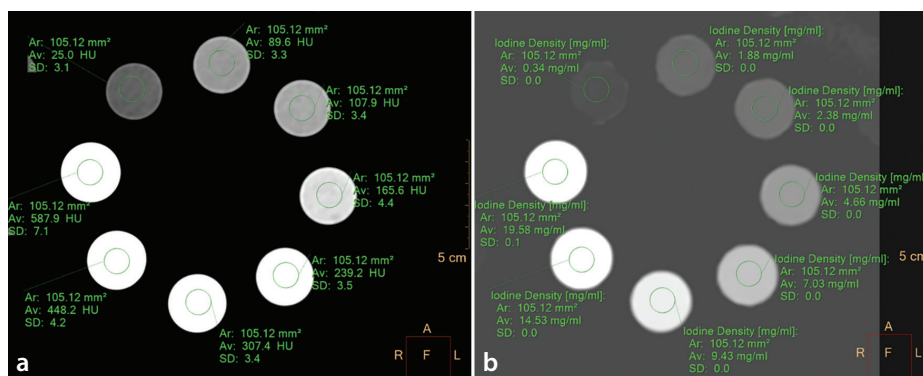


Figure 6. Example of iodine quantification with iodine concentration phantom. For 2–20 mgI/mL concentrations, measured mean computed tomography (CT) attenuation and iodine concentration were documented adjacent to each region of interest on the conventional CT image [(a): window level/width 60/300 HU] and corresponding iodine density map [(b): window level/width 3/15 mgI/mL]. HU, Hounsfield unit.

ditionally, the sample size in these studies ($n = 43$) was relatively small, limiting the determination of correlation coefficients. Furthermore, the DECT-based IC quantification methods lacked validation, especially considering the significant variability that can result from technical factors such as scanner type and body diameter.^{22,23} In contrast, the present study used volumetric quantification in a larger cohort of patients with confirmed hormonal and pathologic diagnosis. As a result, the accuracy of this approach was confirmed in a phantom study, suggesting that the results obtained are more reliable than those reported in previous investigations.^{14–16}

This study appears to be the first volumetric analysis of intrathyroidal IC across three distinct groups defined by differing thyroid hormone levels: hypothyroid, euthyroid, and hyperthyroid. Notably, the results show a statistically significant greater mean reduction in IC in patients with hyperthyroidism compared with those with hypothyroidism. Although the underlying mechanisms for these observed differences remain unclear, several plausible hypotheses can be proposed. For example, Graves' disease (GD), the predominant etiology of hyperthyroidism, is characterized by a two- to threefold increase in thyroid gland weight, accompanied by

markedly increased vascularity, as evidenced by immunohistochemical evaluations of surgical specimens.²⁴ In GD, the interstitial tissue of the thyroid gland is typically infiltrated by lymphocytes, which rapidly lyse thyroglobulin, resulting in thyroid follicular shrinkage or collapse due to colloid deficiency. Conversely, in patients with HT, the lymphocytic infiltration persistently damages the thyroid follicles, culminating in permanent hypothyroidism following an initial phase of hyperthyroidism.²⁴ As HT advances, the thyroid gland undergoes a gradual reduction in size, potentially leading to atrophy in its later stages, which is characterized by extensive fibrosis and a weight reduction to as low as 10–20 g. Therefore, the diminished thyroid volume observed in patients with hypothyroidism within this study may suggest a progression towards the advanced stage of HT. In contrast, the significantly enlarged thyroid glands in patients with hyperthyroidism may be indicative of edematous swelling and increased vascularity, which further diminishes the interstitial compartment of the thyroid parenchyma, as opposed to the predominant fibrosis seen in patients with hypothyroidism.

It is important to note that there is a significant decrease in intrathyroidal IC in patients with pathologically confirmed DTD, even in those who are euthyroid. This observation may suggest a potential precursor to thyroid hormone dysfunction. Additionally, the significant interobserver variability associated with the sonographic diagnosis of DTD must be acknowledged, as well as the limitation that sonographic characteristics alone do not yield quantitative data regarding the functional progression of DTD.^{25,26} In contrast, imaging modalities employed in nuclear medicine, such as thyroid scans and radioactive iodine uptake tests, involve the administration of minimal radiation doses, either intravenously or orally, through the ingestion of the radiopharmaceutical sodium pertechnetate, to evaluate thyroid function. Typically, these assessments are conducted multiple times over a duration ranging from 30 minutes to a maximum of 24 hours.²⁷ Furthermore, DECT-based IC quantification, which does not necessitate the additional use of intravenous contrast, has the potential to provide a comprehensive assessment of both total thyroid volume and intrathyroidal IC as the functional indicators within a relatively brief timeframe.^{14–16} Therefore, this approach may present advantages over conventional CT densitometry, ultrasound, or nuclear medicine imaging in the assessment

of thyroid parenchyma in patients exhibiting thyroid hormone dysfunction or suspected pathological conditions, provided that a radiation dose-optimized DECT scanning protocol is employed.

Nonetheless, our research has primarily focused on intrathyroidal IC quantification. This was achieved through the use of non-contrast DECT images acquired from patients for preoperative staging purposes. Therefore, it is essential to consider several factors that may limit the direct applicability of these findings to the thyroid gland, which is acknowledged as the organ most vulnerable to radiation exposure. First, the DECT technique employed to generate iodine maps, virtual monoenergetic images, and virtual non-contrast images relies on low and high effective X-ray energies to obtain varying attenuation coefficient values for different materials.^{7,8,13} In contrast to other anatomical regions, the thyroid gland, situated in the lower neck, is particularly susceptible to beam-hardening artifacts and image noise during clinical assessments. These factors can considerably compromise the accuracy of DECT-derived iodine maps, as lower-energy photons are absorbed more rapidly than their higher-energy counterparts, resulting in an intensified X-ray beam spectrum by the time it reaches the detector.²⁸ Previous research by Kanatani et al.²⁸ indicated that X-ray beam hardening may lead to an underestimation of CT attenuation in iodine imaging, while the CT attenuation in virtual monoenergetic imaging was found to be overestimated in their phantom study. Although the accuracy of the dual-layer detector DECT utilized in this investigation has been validated in phantom studies for iodine quantification across various scanning and reconstruction parameters, such as tube potential, dose, rotation time, and spectral reconstruction level,^{11,12} there is a lack of published studies specifically addressing the impact of X-ray beam hardening in the vicinity of the thyroid gland. Second, the findings of this study are primarily confined to a specific scanning protocol conducted at a single institution; thus, further research should be undertaken across multiple institutions using different scanners or protocols. Notably, the primary objective of the non-contrast scanning was to identify calcifications in the thyroid gland or cervical lymph nodes, rather than to quantify intrathyroidal IC. Consequently, the technical parameters employed were not optimized to justify the radiation dose, despite their accuracy in

quantifying IC. To effectively assess the advantages of DECT in quantifying IC through DECT-derived iodine maps in thyroid parenchyma, a new CT protocol must be developed to measure relatively low intrathyroidal IC levels, particularly when IC is < 1.0 mgI/mL, in accordance with the principle of radioprotection: “as low as reasonably achievable.” Third, this study retrospectively selected only those patients who consecutively underwent DECT examinations and thyroid function tests. As a result, the majority of participants were middle-aged women with euthyroidism scheduled for thyroid cancer surgery. Additionally, other patients with thyroid hormone dysfunction included in this study were subclinical, presenting as either hypo- or hyperthyroidism, rather than overt disease. Therefore, the relationship between thyroid glandular IC and variables such as age or thyroid function necessitates validation in future studies encompassing a broader range of ages and hormonal statuses. Lastly, this research focused on the intrathyroidal IC quantification by analyzing ROIs within the entire thyroid glands with thyroid nodules measuring 10 mm or less. As a result, the IC of these smaller nodules may have been unintentionally included in the overall analysis, while nodules >1 cm were deliberately excluded. Given the prevalence of thyroid nodules in clinical practice, further studies should be undertaken to assess the impact of nodules on IC quantification, thereby improving the relevance and applicability of the findings.

In conclusion, the application of DECT-based intrathyroidal IC quantification offers a potentially valuable method for investigating iodine metabolism in relation to thyroid hormone disorders. However, further studies are necessary to validate its effectiveness in a more diverse patient population with differing thyroid hormone levels, as well as to develop more rigorous scanning protocols.

Footnotes

Conflict of interest disclosure

The author declared no conflicts of interest.

Funding

This research was supported by Basic Science Research Program through the National Research Foundation of Korea (NRF) funded by the Ministry of Education (2018R1D1A1B07045730). The funder did not have any role in the study design, data collection,

analysis, and interpretation of data, or writing the manuscript.

References

1. Chung HR. Iodine and thyroid function. *Ann Pediatr Endocrinol Metab.* 2014;19(1):8-12. [\[Crossref\]](#)
2. Iida Y, Konishi J, Harioka T, Misaki T, Endo K, Torizuka K. Thyroid CT number and its relationship to iodine concentration. *Radiology.* 1983;147(3):793-795. [\[Crossref\]](#)
3. Imanishi Y, Ehara N, Shinagawa T, et al. Correlation of CT values, iodine concentration, and histological changes in the thyroid. *J Comput Assist Tomogr.* 2000;24(2):322-326. [\[Crossref\]](#)
4. Pandey V, Reis M, Zhou Y. Correlation between computed tomography density and functional status of the thyroid gland. *J Comput Assist Tomogr.* 2016;40(2):316-319. [\[Crossref\]](#)
5. Silverman PM, Newman GE, Korobkin M, Workman JB, Moore AV, Coleman RE. Computed tomography in the evaluation of thyroid disease. *AJR Am J Roentgenol.* 1984;142(5):897-902. [\[Crossref\]](#)
6. Han YM, Kim YC, Park EK, Choe JG. Diagnostic value of CT density in patients with diffusely increased FDG uptake in the thyroid gland on PET/CT images. *AJR Am J Roentgenol.* 2010;195(1):223-228. [\[Crossref\]](#)
7. McCollough CH, Leng S, Yu L, Fletcher JG. Dual- and multi-energy CT: principles, technical approaches, and clinical applications. *Radiology.* 2015;276(3):637-653. [\[Crossref\]](#)
8. Forghani R, De Man B, Gupta R. Dual-energy computed tomography: physical principles, approaches to scanning, usage, and implementation: part 1. *Neuroimaging Clin N Am.* 2017;27(3):371-384. [\[Crossref\]](#)
9. Takeda T, Yu Q, Yashiro T, et al. Iodine imaging in thyroid by fluorescent X-ray CT with 0.05 Mm spatial resolution. *Nucl Instrum Meth A.* 2001;467:1318-1321. [\[Crossref\]](#)
10. Milakovic M, Berg G, Eggertsen R, et al. Determination of intrathyroidal iodine by X-ray fluorescence analysis in 60- to 65-year olds living in an iodine-sufficient area. *J Intern Med.* 2006;260(1):69-75. [\[Crossref\]](#)
11. Duan X, Arbique G, Guild J, Xi Y, Anderson J. Technical note: quantitative accuracy evaluation for spectral images from a detector-based spectral CT scanner using an iodine phantom. *Med Phys.* 2018;45(5):2048-2053. [\[Crossref\]](#)
12. Hua CH, Shapira N, Merchant TE, Klahr P, Yagil Y. Accuracy of electron density, effective atomic number, and iodine concentration determination with a dual-layer dual-energy computed tomography system. *Med Phys.* 2018;45(6):2486-2497. [\[Crossref\]](#)
13. So A, Nicolaou S. Spectral Computed tomography: fundamental principles and

- recent developments. *Korean J Radiol.* 2021;22(1):86-96. [\[Crossref\]](#)
14. Binh DD, Nakajima T, Otake H, Higuchi T, Tsushima Y. Iodine concentration calculated by dual-energy computed tomography (DECT) as a functional parameter to evaluate thyroid metabolism in patients with hyperthyroidism. *BMC Med Imaging.* 2017;17(1):43. [\[Crossref\]](#)
 15. Shao W, Liu J, Liu D. Evaluation of energy spectrum CT for the measurement of thyroid iodine content. *BMC Med Imaging.* 2016;16(1):47. [\[Crossref\]](#)
 16. Li ZT, Zhai R, Liu HM, Wang M, Pan DM. Iodine concentration and content measured by dual-source computed tomography are correlated to thyroid hormone levels in euthyroid patients: a cross-sectional study in China. *BMC Med Imaging.* 2020;20(1):10. [\[Crossref\]](#)
 17. Ha EJ, Chung SR, Na DG, et al. 2021 Korean Thyroid imaging reporting and data system and imaging-based management of thyroid nodules: Korean Society of Thyroid Radiology Consensus Statement and Recommendations. *Korean J Radiol.* 2021;22(12):2094-2123. [\[Crossref\]](#)
 18. Soh SB, Aw TC. Laboratory testing in thyroid conditions - pitfalls and clinical utility. *Ann Lab Med.* 2019;39(1):3-14. [\[Crossref\]](#)
 19. Nikiforov YE, Biddinger PW, Thompson LDR. Diagnostic Pathology and Molecular Genetics of the Thyroid : A Comprehensive Guide for practicing thyroid pathology. 3rd ed., Wolters Kluwer Health; 2018. [\[Crossref\]](#)
 20. User guide for Gammex tissue characterization phantom model 467. [\[Crossref\]](#)
 21. Ahad F, Ganie SA. Iodine, iodine metabolism and iodine deficiency disorders revisited. *Indian J Endocrinol Metab.* 2010;14(1):13-17. [\[Crossref\]](#)
 22. Lennartz S, Parakh A, Cao J, et al. Inter-scan and inter-scanner variation of quantitative dual-energy CT: evaluation with three different scanner types. *Eur Radiol.* 2021;31(7):4438-4451. [\[Crossref\]](#)
 23. Zopfs D, Graffe J, Reimer RP, et al. Quantitative distribution of iodinated contrast media in body computed tomography: data from a large reference cohort. *Eur Radiol.* 2021;31(4):2340-2348. [\[Crossref\]](#)
 24. Bauer DC, McPhee SJ. Thyroid Disease. In: Hammer GD, McPhee SJ, editors. Pathophysiology of Disease: An Introduction to Clinical Medicine, 7e. New York, NY: McGraw-Hill Education; 2013. [\[Crossref\]](#)
 25. Guan H, de Moraes NS, Stuart J, et al. Discordance of serological and sonographic markers for Hashimoto's thyroiditis with gold standard histopathology. *Eur J Endocrinol.* 2019;181(5):539-544. [\[Crossref\]](#)
 26. Ahn HS, Kim DW, Lee YJ, Baek HJ, Ryu JH. Diagnostic accuracy of real-time sonography in differentiating diffuse thyroid disease from normal thyroid parenchyma: a multicenter study. *AJR Am J Roentgenol.* 2018;211(3):649-654. [\[Crossref\]](#)
 27. Spencer CA. Laboratory thyroid tests: a historical perspective. *Thyroid.* 2023;33(4):407-419. [\[Crossref\]](#)
 28. Kanatani R, Shirasaka T, Kojima T, Kato T, Kawakubo M. Influence of beam hardening in dual-energy CT imaging: phantom study for iodine mapping, virtual monoenergetic imaging, and virtual non-contrast imaging. *Eur Radiol Exp.* 2021;5(1):18. [\[Crossref\]](#)